Construction and Building Materials 40 (2013) 812–821

Contents lists available at SciVerse ScienceDirect

Construction and Building Materials

journal homepage: www.elsevier.com/locate/conbuildmat

Application of artificial neural networks to predict the bond strength of FRP-to-concrete joints

Mohammed A. Mashrei *, R. Seracino, M.S. Rahman

Department of Civil, Construction and Environmental Engineering, North Carolina State University, Raleigh, NC 27695-7533, USA

HIGHLIGHTS

- A BPNN model for predicting the bond strength of FRP-to-concrete joints is proposed.
- The results of the BPNN compared with experimental results and those from five existing analytical models.
- BPNN is a convenient tool for developing a parametric study.
- The application of BPNN techniques provide a reliable and simple model for predicting the bond strength.

ARTICLE INFO

Article history:
Received 1 July 2012
Received in revised form 14 November 2012
Accepted 22 November 2012
Available online 28 December 2012

Keywords:
BPNN
FRP
Bond strength
Concrete

ABSTRACT

A Back-Propagation Neural Network (BPNN) model for predicting the bond strength of FRP-to-concrete joints is proposed. Published single-lap shear test specimens were used to predict the bond strength of externally bonded FRP systems adhered to concrete prisms. A database of one hundred and fifty experimental data points from several sources was used for training and testing the BPNN. The data used in the BPNN are arranged in a format of six input parameters including: width of concrete prism; concrete cylinder compressive strength; FRP thickness; bond length; bond width (i.e. FRP width); and FRP modulus of elasticity. The one corresponding output parameter is the bond strength. A parametric study was carried out using BPNN to study the influence of each parameter on the bond strength and to compare results with common existing analytical models. The results of this study indicate that the BPNN provides an efficient alternative method for predicting the bond strength of FRP-to-concrete joints when compared to experimental results and those from existing analytical models.

1. Introduction

A common form of retrofit of existing reinforced concrete (RC) infrastructure is to adhesively bond fiber reinforced polymers (FRPs) to the concrete surfaces [1,2]. During the last few decades, FRP materials have been used in a variety of configurations in the retrofit of existing civil engineering infrastructure, and as an alternative reinforcement for new concrete construction. The attractiveness of the material lies mainly in its corrosion resistance, high strength and stiffness to weight ratio, and fatigue resistance. Further, the high versatility and constructability of the external retrofit techniques using FRP systems results in many advantages in civil and transportation infrastructure applications, since the FRP can be bonded to structures with any cross-section [3].

The strength and ductility of an RC flexural member retrofitted with longitudinal externally bonded (EB) FRP is typically controlled by the intermediate crack (IC) debonding failure mechanism. Because of its relative simplicity, and the similarity of the stress state at the FRP-to-concrete interface, the single-lap shear test [4] shown in Fig. 1 is often used to idealize the critical IC debonding mechanism [5,6]. From the single-lap shear test the debonding mechanism may be better understood, the bond strength quantified, and the fundamental interface bond stress–slip relationship determined, which is required in analytical and numerical simulation [7].

Many experimental studies have been conducted to investigate the bond strength using the single-lap shear tests [4,5,8–12]. Also, many theoretical studies have been published using various methods such as fracture mechanics, the finite element method, and empirically derived equations [4,6–8,13–18] to study the bond strength of FRP-to-concrete joints. Conventional modeling often tends to become quite intractable and difficult. Many of the models used to estimate the bond strength of FRP-to-concrete joints are highly empirical and their predictive abilities are limited by the

* Corresponding author.
E-mail addresses: moha74ed@yahoo.com, mamashre@ncsu.edu (M.A. Mashrei), rudi_seracino@ncsu.edu (R. Seracino), rahman@ncsu.edu (M.S. Rahman).

0950-0618/$ - see front matter © 2012 Elsevier Ltd. All rights reserved.
http://dx.doi.org/10.1016/j.conbuildmat.2012.11.109

Nomenclature

b_c	width of concrete prism	P_u	bond strength
b_f	width of FRP	s_f	local slip when bond stress reduces to zero
E_f	elastic modulus of FRP	s_o	local slip at maximum bond stress
E_c	elastic modulus of concrete	t_a	thickness of adhesive layer
f'_c	concrete cylinder compressive strength	t_d	thickness of debonded concrete
f_t	concrete tensile strength	t_f	thickness of FRP
G_f	interfacial fracture energy	α	reduction factor
G_{cf}	fracture energy of concrete	β_l	bond length factor
K_G	factor of the debonding capacity model	β_w	width ratio factor
k_c	concrete compaction factor	τ_{max}	maximum local bond stress
L	bond length	τ'	thickness ratio of debonded concrete cover and FRP
L_e	effective bond length	Σ	Young's modulus ratio of FRP and concrete

corresponding data sets from which they were derived. In some cases, the models do not provide reliable predictions for use in practice. In recent years, alternative approaches to modeling have emerged under soft computing, such as neural networks (NNs). NNs are an observational model developed on the basis of available data representing a mapping between input and output variables. The main advantage of NNs is that one does not have to explicitly assume a model form, which is a prerequisite in the conventional approaches [19]. In other words, when the information available for constructing the model is only available in the form of data derived from observations or measurements, neural network models, based on the input/output variables system, have been successfully used to generate the relationships between these variables.

NNs are a system of interconnected computational neurons arranged in an organized fashion to carry out an extensive computing to perform a mathematical mapping [20]. First interest in NNs (or parallel distributed processing) emerged after the introduction of simplified neurons by McCulloch and Pitts in 1943 [21]. These neurons were presented as models of biological neurons and as conceptual components for circuits that could perform computational works. NNs can be most adequately characterized as a computational model with particular properties such as the ability to adapt or learn, to generalize, and to cluster or organize data, in which operation is based on parallel processing.

NN models have a large number of highly interconnected processing elements (nodes or units) that usually operate in parallel and are configured in regular architectures. The collective behavior of an NN, like a human brain, demonstrates the ability to learn, recall, and generalize from training patterns or data. NNs are inspired by modeling networks of biological neurons in the brain. Hence, the processing elements in NNs are also called artificial neurons [20,22]. More information on the use of NNs in engineering applications may be found in [22]. The NN used in this paper is typically applied to solve many civil engineering applications such as structural analysis and design [23–25], structural damage assessment [26,27], structural dynamics and control, seismic liquefaction prediction, constitutive modeling [28,29] and pavement condition-rating modeling [30].

The purpose of this paper is to investigate the ability of an NN to predict the bond strength of FRP-to-concrete joints. The performance of the NN model is compared with experimental data and other published analytical models. The study is based on an available database including 150 test specimens.

2. Fundamental aspects of artificial neural networks

Unlike conventional problem solving algorithms, neural networks can be trained to perform a particular task. This is done by presenting the system with a representative set of examples describing the problem, namely pairs of input and output samples; the neural network will then extrapolate the mapping between input and output data. After training, the neural network can be used to recognize data that is similar to any of the examples shown during the training phase [22]. The neural network can even recognize incomplete or noisy data, an important feature that is often used for prediction, diagnosis or control purposes. Further, neural

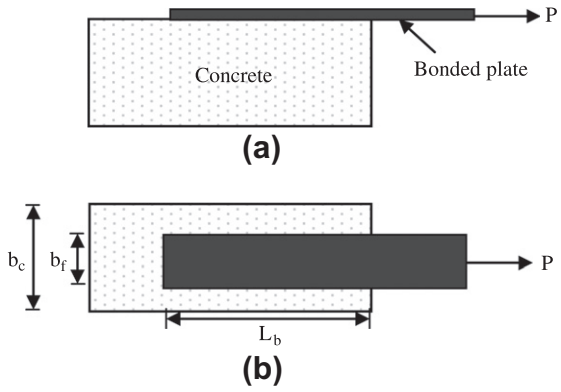

Fig. 1. Single-lap shear test specimen (a) side view (b) top view.

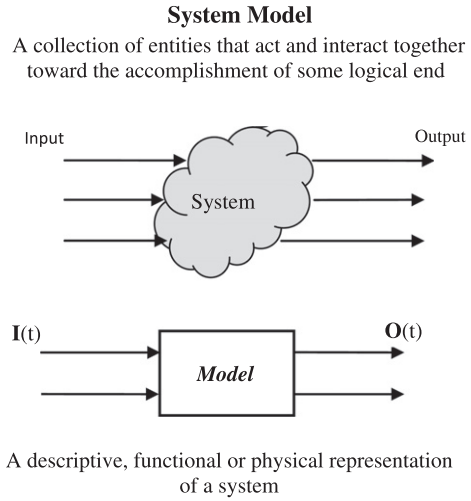

Fig. 2. Schematic diagram of a system model [31].

networks have the ability to self-organize, therefore enabling segmentation or coarse coding of data. A model is an abstraction that behaves somewhat like a defined "system". In the real world, a system is a set of transformations that convert input states into output states. The key is that it converts input into output through some defined set of algorithms as shown schematically in Fig. 2 [31].

In general a typical neural network model consists of: (i) an input layer, where input data are presented to the network; (ii) an output layer, which comprises neurons representing target variables; and (iii) one or more hidden intermediate layers. The neural network has a parallel distributed architecture with a large number of nodes and connections with varying weights. Each node has a computation process; multiplying its weight by each input, summation of their product, and then using the activation function to produce the actual output [32].

The commonly used Back-Propagation Neural Networks (BPNNs) are trained by feeding a data set of input and target variables. The main objective of training the neural network is to update the connection weights to reduce the errors between the actual output values and target output values to a satisfactory level. This process is carried out through the minimization of the defined error function using an update method. Also, the determination of the number of hidden layers, number of hidden nodes, transfer functions, and normalization of data are considered to get the best performance of the model. At the end of the training phase, the neural network represents a model that should be able to predict the target value given for the input pattern. After the errors are minimized, the associated trained weights of the model are tested with a separate set of testing data that was not used in training [22]. The resilient function with BPNN training algorithm is used in this study. Details of the architecture and procedures of BPNN are described elsewhere in the available literature [22,33]. A multilayer network typically uses sigmoid transfer functions in the hidden layers. These functions are often called "squashing" functions, since they compress an infinite input range into a finite output range. Sigmoid functions are characterized by the fact that their slope must approach zero, as the input gets large. These may cause a problem when using steepest descent to train a multilayer network, since more of training function such as the gradient can have a very small magnitude; and therefore, cause small changes in the weights and biases, even though the weights and biases are far from their optimal values [32].

The aim of the resilient function in the training process is to eliminate these harmful effects of the magnitudes of the partial derivatives. Only the sign of the derivative is used to determine the direction of the weight update; the magnitude of the derivative has no effect on the weight update [32]. The use of resilient function in training is generally much faster than the standard steepest descent algorithm. It also has the benefit that it requires only a modest increase in memory requirements, as it only needs to store the update values for each weight and bias, which is similar to storage of the gradient [32].

3. Existing models to predict bond strength of FRP-to-concrete joints

Many models have been published in the open literature to theoretically predict the bond strength of FRP-to-concrete joints. A brief summary of five models are given in the following. The first three models presented come from relatively recent publications that were compared to more than fifteen other well-known models and hundreds of experimental FRP-to-concrete joint tests to demonstrate their predictive abilities. The latter two models come from international design guides on FRP strengthening of concrete structures. Specific details of the models including their derivation and comparisons against other models and experimental data may be found in the references cited. It is worth noting that all the models have the same form, that is, the bond strength P_u is a function of the bond width (equal to the width of the FRP b_f for the EB retrofit case), the axial rigidity of the FRP system $E_f t_f$, and some measure of fracture energy. Further, in all of the models it is assumed that the concrete substrate is well prepared and the quality of the bond is such that debonding will occur within the first few millimeters of the concrete substrate. For convenience, all variables are defined in the Nomenclature.

3.1. Lu et al. [13]

Lu et al. [13] proposed a bond strength model of FRP-to-concrete bonded joints in terms of the interfacial fracture energy based on finite element predictions as follows, where the bond strength is a function of the bonded length, L

$$P_u = \beta_l b_f \sqrt{2E_f t_f G_f} \tag{1}$$

where

$$\beta_l = \begin{cases} 1 & \text{if } L \geq L_e \\ \dfrac{L}{L_e}\left(2 - \dfrac{L}{L_e}\right) & \text{if } L < L_e \end{cases}$$

$$L_e = a + \frac{1}{2\lambda_1} \ln\left[\frac{\lambda_1 + \tan(\lambda_2 a)}{\lambda_1 - \tan(\lambda_2 a)}\right]$$

$$G_f = 0.308\beta_w^2 \sqrt{f_t}$$

$$\lambda_1 = \sqrt{\frac{\lambda_{max}}{s_o E_f t_f}}$$

$$\lambda_{max} = 1.5\beta_w f_t$$

$$\lambda_2 = \sqrt{\frac{\lambda_{max}}{(s_f - s_o)E_f t_f}}$$

$$S_o = 0.0195\beta_w f_t$$

$$S_f = \frac{2G_f}{\lambda_{max}}$$

$$a = \frac{1}{\lambda_2} arcsin\left[0.99\sqrt{\frac{(s_f - s_o)}{s_f}}\right]$$

and,

$$\beta_w = \sqrt{\frac{2.25 - b_f/b_c}{1.25 + b_f/b_c}}$$

3.2. Dai et al. [34]

Dai et al. [34] proposed a maximum bond strength model (where it must be assumed that the bonded length L is greater than the effective length L_e) based on the interfacial fracture energy and stiffness of FRP given by:

$$P_u = (b_f + 2\Delta b_f)\sqrt{2E_f t_f G_f} \tag{2}$$

where

$$G_f = 0.254(f_c')^{0.236}$$

and $\Delta b_f = 3.7$ mm is based on experimental analysis.

3.3. Wu et al. [7]

Wu et al. [7] presented a model based on fracture mechanics theory for laminated structures, and proposed the following model which, similar to the Dai et al. [34] model, is also not a function of effective bond length L_e

$$P_u = \beta_w b_f \sqrt{2\left(1+\frac{\lambda'}{\Sigma}\right)E_f t_f G_{cf}} \quad (3)$$

where

$$\beta_w = \sqrt{\frac{2-b_f/b_c}{1+b_f/b_c}}$$

$\lambda' = t_d/t_f$

$t_d = 3.5$ mm

$\Sigma = E_f/E_c$

and, G_{cf} is taken 0.17 N/mm.

3.4. fib model [35]

Holzenkamfer's model [36], as modified by Neubauer and Rostasy [14], is adopted by the international federation for structural concrete (*fib*) to estimate the bond strength of FRP-to-concrete joints as given by

$$P_u = \begin{cases} 0.64\ \alpha k_c \beta_w b_f \sqrt{E_f t_f f_t} & \text{if } L \geq L_e \\ 0.64\ \alpha k_c \beta_w b_f \sqrt{E_f t_f f_t}\,\frac{L}{L_e}\left(2-\frac{L}{L_e}\right) & \text{if } L \geq L_e \end{cases} \quad (4)$$

where

$$\beta_w = 1.06\sqrt{\frac{2-b_f/b_c}{1+b_f/400}} \geq 1$$

$$L_e = \sqrt{\frac{E_f t_f}{2f_t}}$$

$\alpha = 1.0$ and, $k_c = 1.0$.

3.5. CNR-DT200/2004 model [37]

The bond strength according to CNR-DT200/2004 [37] can be computed using the following expressions:

$$P_u = b_f \sqrt{2E_f t_f K_G \beta_w \beta_l \sqrt{f'_c f_c}} \quad (5)$$

where

$K_G = 0.03$

$$\beta_l = \begin{cases} 1 & \text{if } L \geq L_e \\ \frac{L}{L_e}\left(2-\frac{L}{L_e}\right) & \text{if } L < L_e \end{cases}$$

$$L_e = \sqrt{\frac{E_f t_f}{2f_t}}$$

$\beta_w = \sqrt{\frac{2-b_f/b_c}{1+b_f/400}} \geq 1$ with $b_f/b_c \geqslant 0.33$. If $b_f/b_c < 0.33$, then the value of β_w is determined using $b_f/b_c = 0.33$

Table 1
Range of input parameters in the database.

Parameter	Range
Width of prism (b_c)	100–228 mm
Concrete cylinder compressive strength (f'_c)	16–50 MPa
Width of FRP (b_f)	10–100 mm
Thickness of FRP (t_f)	0.08–1.4 mm
Modulus of elasticity of FRP (E_f)	83–300 GPa
Bond length (L)	50–300 mm

4. Modeling of bond strength of FRP-to-concrete joints using BPNN

4.1. Description of experimental database

In this study, the experimental database includes 150 carbon FRP-to-concrete joint test specimens, which are compiled from several sources [4,5,8–12,18]. Details of the database used to train and test the BPNN are summarized in Appendix A. Table 1 summarizes the ranges of the input variables. All specimens are single-lap shear tests and all specimens failed by debonding in the concrete substrate. Among all the specimens in the database, 125 (83%) were randomly selected and used as training sets, and the remaining 25 (17%) are used to investigate the accuracy of the trained network.

4.2. Architecture of the BPNN model

The Neural Network Toolbox [32] of MATLAB was used to develop the BPNN. The selection of input variables for building the BPNN model was guided by the significance of key parameters on the bond strength as determined from existing experimental results and analytical models, as mentioned previously.

A sigmoid function was considered as an activation function for all processing elements in the input and hidden layers, and a linear function was used for the output layer. The number of hidden layers, neurons, and epochs must be specified to start the network training. After a trial and error procedure a network of two hidden layers with five neurons in each layer was selected, which minimized the mean square error (MSE). The network was trained continually through updating of the weights until a final error of 5.9×10^{-3} was achieved after 200 epochs. Fig. 3 shows the performance of the training and testing data sets.

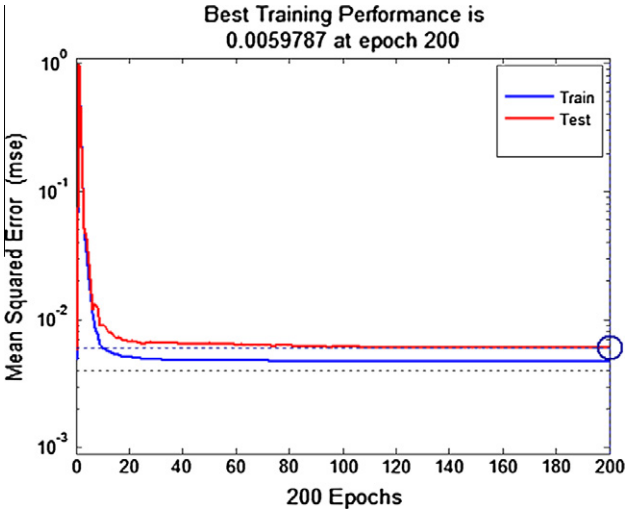

Fig. 3. Convergence of the BPNN for training and testing data sets.

4.3. Graphical user interface of the BPNN

A graphical user interface (GUI) was developed for the BPNN program to provide a user-friendly platform to run the analysis using intuitive text boxes. The GUI represents a simplified tool by which the developed neural network can be used to predict the bond strength of a given FRP-to-concrete joint. A window is provided through which the input data is entered and the results of the analysis are displayed. The results include the output of the network and the regression analysis for both the training and testing data sets. The main advantage of the GUI is in its simplicity and the negligible time required to predict the bond strength.

5. Results and discussion

The predictive capability of the BPNN was compared to the training and testing data sets, as shown in Figs. 4 and 5, respectively. It can be seen that the predicted values were found to be in close agreement with the experimental (target) values where the correlation factors (R) for both the training and testing data sets are 0.99.

After validating the BPNN, a parametric study can be easily undertaken to assess, for example, the sensitivity of bond strength on the selected input parameters. To this end, the predictions of the BPNN are compared to the same for the five existing models previously presented. In Figs. 6–10 the reference FRP-to-concrete joint has the following material and geometric properties, b_f = 40 - mm, b_c = 160 mm, t_f = 0.84, t_f = 35 MPa, L = 150 mm and E_f = 180 - GPa, which are all within the range of values obtained from the experimental database as given in Table 1. The influence of the bond width b_f on the bond strength is presented in Fig. 6. As expected, it can be seen that increasing b_f increases the bond strength. The trend is similar for all models considered, but there is significant variability in the predicted bond strength. From Fig. 7 it can be concluded that the bond strength increases with increasing f_c' however, the influence is not strong. The trend is similar among all models but again, the range of predicted strength varies by a factor of 2. In Fig. 8 the bond strength is plotted against the FRP thickness t_f where it can be seen that increasing t_f increases the bond strength, as expected, but at a decreasing rate. Fig. 9 compares the bond strength against the bond length L where it can be seen that for those models that explicitly consider bond length less than an effective length L_e, the bond strength increases up to approximately L = 150 mm (for this particular FRP-to-concrete joint) after which all models except the BPNN assume a constant bond strength. Interestingly, the BPNN predicts a slight decrease in strength beyond this bonded length which is in fact in agreement with some of the experimental results in the database. Unlike internal reinforcing, increasing the bonded length of EB FRP reinforcement does not necessarily allow the tensile force in the reinforcement to increase until FRP rupture. However, increased bond length provides a more ductile debonding behavior prior to complete detachment of the FRP reinforcement [12]. Finally, the sensitivity of the bond strength to the elastic modulus of the FRP E_f is illustrated in Fig. 10 where it can be seen that the bond strength increases with increasing E_f. Again, the trend is similar for all models but there is an almost twofold range of predicted bond strength.

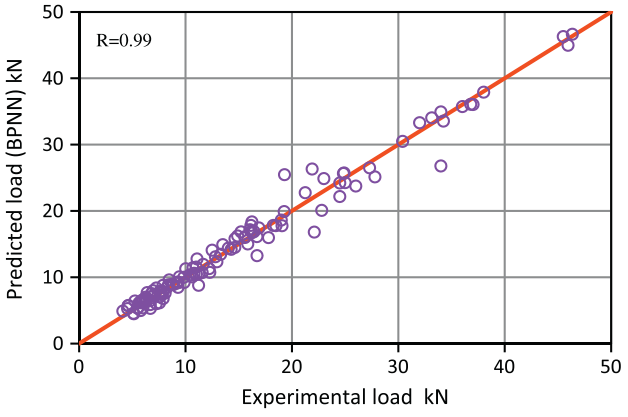

Fig. 4. BPNN bond strength for training data set.

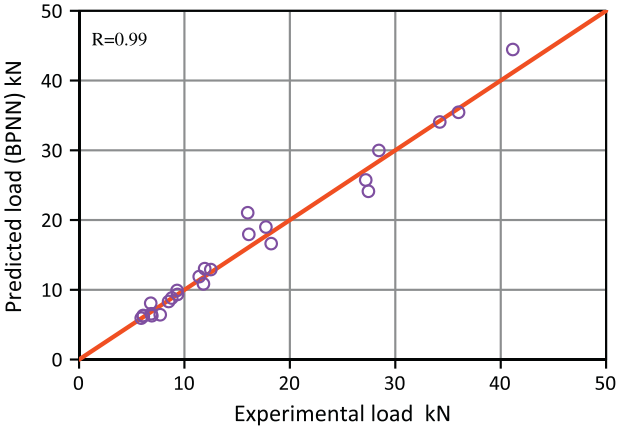

Fig. 5. BPNN bond strength for testing data set.

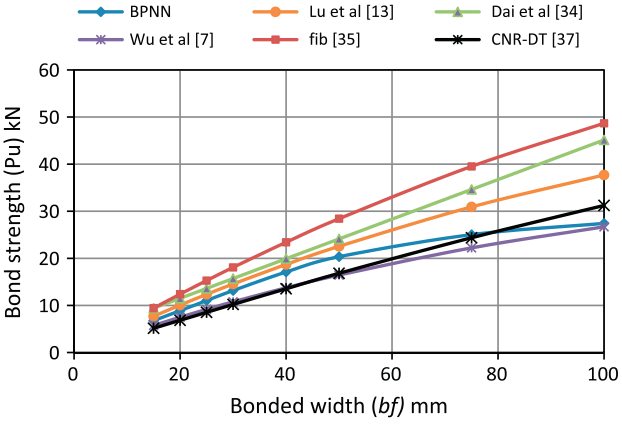

Fig. 6. Effect of bonded width on bond strength.

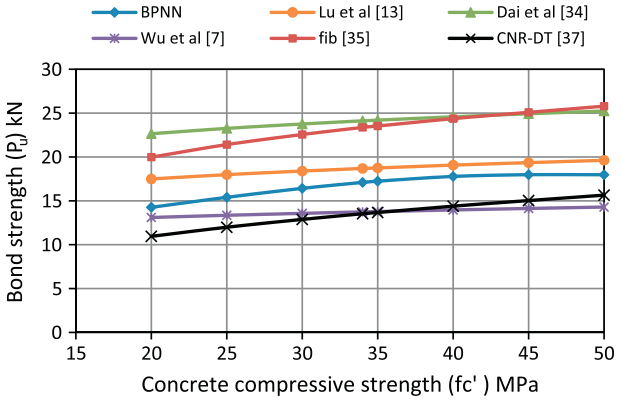

Fig. 7. Effect of concrete compressive strength on bond strength.

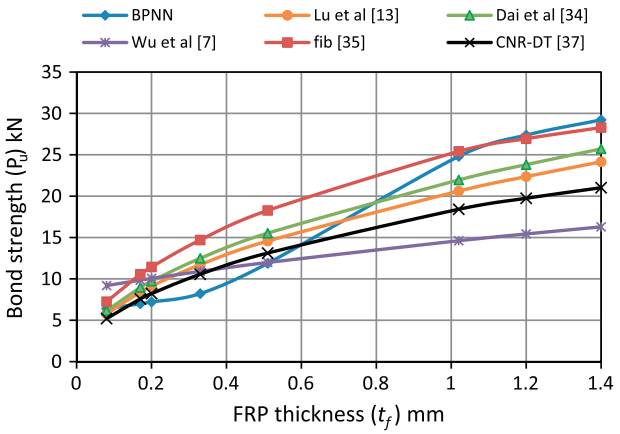

Fig. 8. Effect of FRP thickness on bond strength.

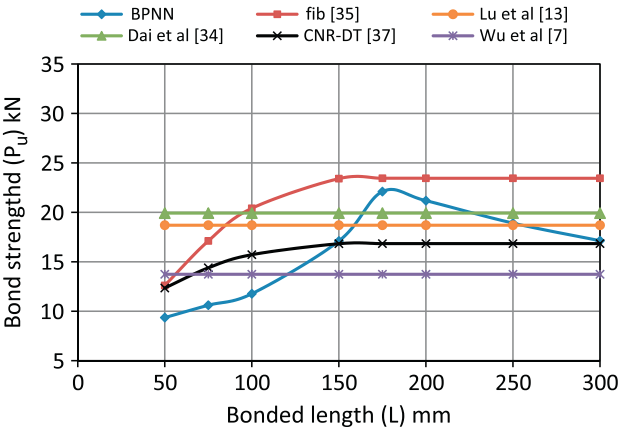

Fig. 9. Effect of bonded length on bond strength.

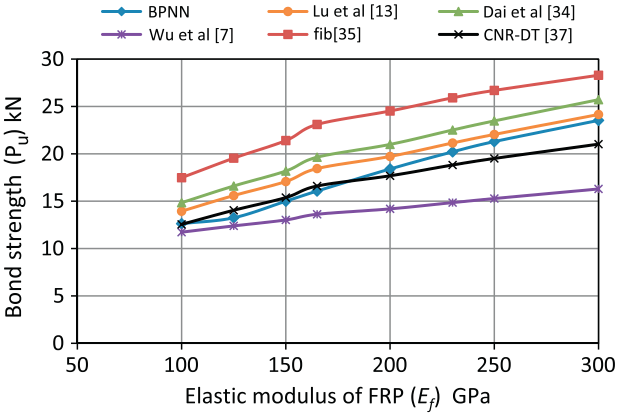

Fig. 10. Effect of elastic modulus of FRP on bond strength.

Table 2
Relative importance (RI) of BPNN model.

Input variables	b_c (mm)	f'_c (MPa)	b_f (mm)	t_f(mm)	E_f(GPa)	L(mm)
RI (%)	16.5	9.7	14.7	22.6	20.4	16.1

The relative importance (RI) of each parameter on the bond strength of FRP-to-concrete joints, based on the predictions of

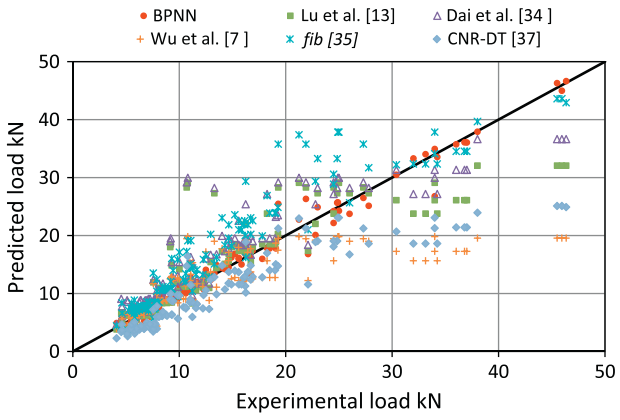

Fig. 11. Experimental versus predicted bond strength for training data set.

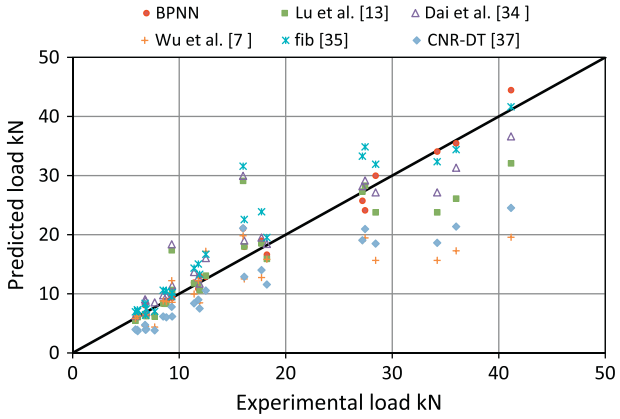

Fig. 12. Experimental versus predicted bond strength for testing data set.

the BPNN, is provided in Table 2 using the methodology suggested by Garson [38]. After training all the data sets with the final model, the relative importance of each input variable may be determined. In this method the connection weights from the input layer to the hidden nodes in hidden layer(s) to the output layer are used to partition the relative share of the output prediction associated with each input variable. It is clear that the terms associated with the axial rigidity of the EB FRP reinforcement have a significant impact on the bond strength. Conversely, the concrete compressive strength has the lowest impact, which is explained by the fact that debonding cracks develop when the principal tensile stress reaches the concrete tensile strength that is a function of $f_c'^{0.5}$ and hence, is less sensitive to changes in compression strength.

6. BPNN prediction comparison with existing models

The ability of the BPNN to predict the bond strength of FRP-to-concrete joints is compared to the five existing models previously presented. The predictions of all the models including the BPNN are plotted against the experimental data for the training and testing data sets in Figs. 11 and 12, respectively. Table 3 summarizes the average and standard deviation of the ratio of the experimental bond strength (P_e) to the predicted (P_i) for the training and testing data sets separately, where a ratio less than unity indicates an unconservative prediction. The BPNN gives an average ratio for training and testing data sets of 1.0 and 0.99, with standard deviations of 0.1 and 0.09, respectively. These values indicate that the proposed BPNN can predict more accurately and reliably the bond strength compared to the other five models. Table 4 confirms

Table 3
Comparison of bond strength prediction.

Model	Average P_e/P_i		STDEV P_e/P_i	
	Training	Testing	Training	Testing
BPNN	1.00	0.99	0.10	0.09
Lu et al. [13]	0.98	1.04	0.21	0.20
Dai et al. [34]	0.85	0.90	0.18	0.17
Wu et al. [7]	1.21	1.30	0.41	0.42
fib [35]	0.83	0.87	0.17	0.13
CNR-DT2000/2004 [37]	1.40	1.48	0.29	0.26

Table 4
Comparison of correlation coefficient, *R*.

Model	*R*	
	Training	Testing
BPNN	0.99	0.99
Lu et. al. [12]	0.87	0.89
Dai et al. [34]	0.90	0.92
Wu et al. [7]	0.77	0.80
fib [35]	0.93	0.94
CNR-DT2000/2004 [37]	0.91	0.92

this conclusion when comparing the correlation factor coefficient for all models for both training and testing data sets. Values of 0.99 for the BPNN training and testing data sets are close to unity and better than that of the other models.

7. Conclusions

This study can be considered as a contribution to ongoing efforts to apply neural networks for solving structural engineering problems. In this paper the application of the neural network technique to predict the bond strength of FRP-to-concrete joints has been demonstrated using 150 test specimens collected from different sources. A BPNN model with six input nodes, two hidden layers, five nodes in each hidden layer and one output node (which is the bond strength) was developed. A graphical user interface (GUI) was developed for the BPNN. The GUI provides a fast and easy-to-use tool to apply the developed neural network in the prediction of bond strength for new FRP-to-concrete joints. The predicted bond strength from the BPNN model was found to agree better with experimental data than the existing five models considered. It can also be concluded that the BPNN is a convenient tool for developing a parametric study among several parameters that affect the physical phenomenon in engineering problems.

This study shows the potential of neural networks as a tool to support the work of structural engineers in the modeling and prediction of bond strength of FRP-to-concrete joints. Therefore, it is believed that the application of neural network techniques may provide reliable and simple models for other prediction problems in structural engineering.

Appendix A

See Table A.

Table A
Experimental database used to construct the BPNN model.

No.	b_c (mm)	f'_c (MPa)	b_f (mm)	t_f (mm)	E_f (GPa)	L (mm)	P_u (kN)	Reference
1	100	29.7	50	1.2	165	100	18.25	Sharma et al. [8]
2	100	29.7	50	1.2	165	130	24.5	
3	100	29.7	50	1.2	165	150	28.44	
4	100	29.7	50	1.2	165	175	32.00	
5	100	29.7	50	1.2	165	200	34.22	
6	100	29.7	50	1.2	165	250	33.14	
7	100	29.7	50	1.2	165	300	34.24	
8	100	35.8	50	1.2	210	150	30.40	
9	100	35.8	50	1.2	210	180	34	
10	100	35.8	50	1.2	210	190	36	
11	100	35.8	50	1.2	210	200	36.02	
12	100	35.8	50	1.2	210	230	37.02	
13	100	35.8	50	1.2	210	255	36.8	
14	100	29.7	50	1.2	300	160	38.02	
15	100	29.7	50	1.2	300	180	41.15	
16	100	29.7	50	1.2	300	200	46.35	
17	100	29.7	50	1.2	300	250	45.5	
18	100	29.7	50	1.2	300	300	45.95	
19	150	23	25	0.17	256	75	5.24	Yao et al. [5]
20	150	23	25	0.17	256	85	5.85	
21	150	23	25	0.17	256	95	6	
22	150	23	25	0.17	256	115	6.08	
23	150	23	25	0.17	256	145	6.11	
24	150	23	25	0.17	256	190	6.69	
25	150	27.1	25	0.17	256	100	5.94	
26	150	27.1	50	0.17	256	100	11.66	
27	150	27.1	75	0.17	256	100	14.63	
28	150	27.1	100	0.17	256	100	19.07	
29	150	18.9	25	0.17	256	95	5.64	
30	150	19.8	25	0.17	256	95	6.10	
31	150	21.1	15	0.17	256	95	4.11	
32	150	21.1	25	0.17	256	95	6.26	
33	150	21.1	50	0.17	256	95	12.22	
34	150	21.1	75	0.17	256	95	14.29	
35	150	21.1	100	0.17	256	95	15.58	
36	150	24.9	25	0.17	256	95	6.71	

Table A (*continued*)

No.	b_c (mm)	f'_c (MPa)	b_f (mm)	t_f (mm)	E_f (GPa)	L (mm)	P_u (kN)	Reference
37	150	24.9	25	0.17	256	145	6.91	
38	150	24.9	25	0.17	256	190	7.26	
39	150	24.9	25	0.17	256	240	6.7	
40	100	28.88	40	0.17	230	100	8.75	Takeo et al. [10]
41	100	26.66	40	0.17	230	100	8.85	
42	100	28.88	40	0.17	230	200	9.30	
43	100	26.66	40	0.17	230	200	8.50	
44	100	28.88	40	0.17	230	300	9.30	
45	100	26.66	40	0.17	230	300	8.30	
46	100	24.99	40	0.17	230	100	8.80	
47	100	26.17	40	0.17	230	100	8.41	
48	100	24.4	40	0.17	230	100	7.89	
49	100	24.99	40	0.33	230	100	11.4	
50	100	24.99	40	0.5	230	100	13.5	
51	100	24.4	40	0.17	230	100	11.23	
52	100	49.97	40	0.17	230	100	7.9	
53	100	24.99	40	0.11	230	100	7.7	
54	100	26.17	40	0.11	230	100	6.95	
55	200	17	50	0.42	110	100	7.56	Toutanji et al. [18]
56	200	17	50	0.66	110	100	9.29	
57	200	30	10	1.4	152.2	50	5.15	Woo and Yun [12]
58	200	30	10	1.4	152.2	100	7.55	
59	200	30	10	1.4	152.2	150	7.7	
60	200	30	10	1.4	152.2	200	7.9	
61	200	30	10	1.4	152.2	250	6.25	
62	200	30	10	1.4	152.2	300	7.58	
63	200	40	10	1.4	152.2	50	5.1	
64	200	40	10	1.4	152.2	100	6.85	
65	200	40	10	1.4	152.2	150	6.35	
66	200	40	10	1.4	152.2	200	6.95	
67	200	40	10	1.4	152.2	250	6.8	
68	200	40	10	1.4	152.2	300	6.4	
69	200	50	10	1.4	152.2	50	4.55	
70	200	50	10	1.4	152.2	100	7.1	
71	200	50	10	1.4	152.2	150	7.78	
72	200	50	10	1.4	152.2	200	7.65	
73	200	50	10	1.4	152.2	250	6.8	
74	200	50	10	1.4	152.2	300	7.25	
75	200	30	30	1.4	152.2	50	9.3	
76	200	30	30	1.4	152.2	100	16.25	
77	200	30	30	1.4	152.2	150	16.2	
78	200	30	30	1.4	152.2	200	22.1	
79	200	30	30	1.4	152.2	250	15.6	
80	200	30	30	1.4	152.2	300	15.85	
81	200	40	30	1.4	152.2	50	9.15	
82	200	40	30	1.4	152.2	100	14.9	
83	200	40	30	1.4	152.2	150	16.05	
84	200	40	30	1.4	152.2	200	16.15	
85	200	40	30	1.4	152.2	250	16.11	
86	200	40	30	1.4	152.2	300	16.9	
87	200	50	30	1.4	152.2	50	9.2	
88	200	50	30	1.4	152.2	100	17.8	
89	200	50	30	1.4	152.2	150	15.22	
90	200	50	30	1.4	152.2	200	18.5	
91	200	50	30	1.4	152.2	250	19	
92	200	50	30	1.4	152.2	300	17.73	
93	200	30	50	1.4	152.2	50	13.3	
94	200	30	50	1.4	152.2	100	26	
95	200	30	50	1.4	152.2	150	27.8	
96	200	30	50	1.4	152.2	200	27.2	
97	200	30	50	1.4	152.2	250	24.84	
98	200	30	50	1.4	152.2	300	23	
99	200	40	50	1.4	152.2	50	10.7	
100	200	40	50	1.4	152.2	100	24.5	
101	200	40	50	1.4	152.2	150	27.45	
102	200	40	50	1.4	152.2	200	19.3	
103	200	40	50	1.4	152.2	250	21.9	
104	200	40	50	1.4	152.2	300	27.3	
105	200	50	50	1.4	152.2	50	10.8	
106	200	50	50	1.4	152.2	100	16	
107	200	50	50	1.4	152.2	150	21.25	
108	200	50	50	1.4	152.2	200	25	
109	200	50	50	1.4	152.2	250	24.9	
110	200	50	50	1.4	152.2	300	34	

(*continued on next page*)

Table A (*continued*)

No.	b_c (mm)	f'_c (MPa)	b_f (mm)	t_f (mm)	E_f (GPa)	L (mm)	P_u (kN)	Reference
111	228.2	36.1	25.4	1.02	106	76.2	8.46	Chajes et al. [4]
112	228.2	47.1	25.4	1.02	106	76.2	10.4	
113	228.2	43.6	25.4	1.02	106	76.2	10.62	
114	228.2	24.1	25.4	1.02	106	76.2	9.87	
115	228.2	28.9	25.4	1.02	106	76.2	9.34	
116	228.2	36.4	25.4	1.02	106	50.8	8.09	
117	228.2	36.4	25.4	1.02	106	101.6	12.81	
118	152.4	36.4	25.4	1.02	106	152.4	11.92	
119	152.4	36.4	25.4	1.02	106	203.2	11.57	
120	150	16	100	0.08	240	100	11.0	Zhao et al. [11]
121	150	16	100	0.08	240	150	11.25	
122	150	28.63	100	0.08	240	100	12.5	
123	150	28.63	100	0.08	240	150	12.5	
124	150	22.39	20	0.51	83.03	150	5.81	Ren [9]
125	150	22.39	50	0.51	83.03	150	10.6	
126	150	22.39	80	0.51	83.03	150	18.23	
127	150	35.33	20	0.51	83.03	100	4.63	
128	150	35.33	20	0.51	83.03	150	5.77	
129	150	35.33	50	0.51	83.03	60	9.42	
130	150	35.33	50	0.51	83.03	100	11.03	
131	150	35.33	50	0.51	83.03	150	11.8	
132	150	35.33	80	0.51	83.03	100	14.65	
133	150	35.33	80	0.51	83.03	150	16.44	
134	150	43.29	20	0.51	83.03	100	5.99	
135	150	43.29	20	0.51	83.03	150	5.9	
136	150	43.29	50	0.51	83.03	100	9.84	
137	150	43.29	50	0.51	83.03	150	12.28	
138	150	43.29	80	0.51	83.03	100	14.02	
139	150	43.29	80	0.51	83.03	150	16.71	
140	150	22.39	20	0.33	207	150	5.48	
141	150	22.39	50	0.33	207	150	10.02	
142	150	22.39	80	0.33	207	150	19.27	
143	150	35.33	20	0.33	207	100	5.54	
144	150	35.33	20	0.33	207	150	4.61	
145	150	35.33	50	0.33	207	100	11.08	
146	150	43.29	20	0.33	207	100	5.78	
147	150	43.29	50	0.33	207	100	12.95	
148	150	43.29	50	0.33	207	150	16.72	
149	150	43.29	80	0.33	207	100	16.24	
150	150	43.29	80	0.33	207	150	22.8	

References

[1] Oehlers DJ, Seracino R. Design of FRP and steel plated RC structures. Elsevier Science; 2004. ISBN:978008044548.

[2] Teng J, Chen J, Smith S, Lam L. FRP-strengthened RC structures. Wiley; 2002. ISBN:047148706.

[3] Wu Z, Yoshizawa H. Analytical/experimental study on composite behavior in strengthening structures with bonded carbon fiber sheets. J Reinf Plast Compos 1999;18(12):1131–55.

[4] Chajes M, William F, Januszka T, Thomson T. Bond and force transfer of composite material plates bonded to concrete. ACI Struct J 1996;93(2):208–17.

[5] Yao J, Teng JG, Chen JF. Experimental study on FRP-to-concrete bonded joints. J Compos Part B: Eng 2005;36(2):99–113.

[6] Chen JF, Teng JG. Anchorage strength for FRP and steel plates bonded to concrete. J Struct Eng 2001;127(5):784–91.

[7] Wu Y, Zhou Z, Yang Q, Chen W. On shear bond strength of FRP-concrete structures. J Eng Struct 2010;32:897–905.

[8] Sharma SK, Mohamed MS, Goldar D, Sikdar PK. Plate–concrete interfacial bond strength of FRP and metallic plated concrete specimens. J Compos Part B: Eng 2006;37:54–63.

[9] Ren H. Study on basic theories and long time behavior of concrete structure strengthening by fiber reinforced polymer. PhD thesis, Dalian University of Technology, China; 2003.

[10] Takeo K, Matsushita H, Makizumi T, Nagashima G. Bond characteristics of CFRP sheets in the CFRP bonding technique. In: Proc. of Japan Concrete Institute; 1997;19(2):1599–1604.

[11] Zhao HD, Zhang Y, Zhao M. Research on the bond performance between CFRP plate and concrete. In: Proc. of 1st conference on FRP concrete structures of China; 2000: p. 247–253.

[12] Woo SK, Lee Y. Experimental study on interfacial behavior of CFRP-bonded concrete. J Civil Eng 2010;14(3):385–93.

[13] Lu XZ, Teng JG, Ye LP, Jiang JJ. Bond-slip models for FRP sheets/plates bonded to concrete. J Eng Struct 2005;27(6):920–37.

[14] Neubauer U, Rostásy FS. Design aspects of concrete structures strengthened with externally bonded CFRP plates. In: Proceedings of 7th international conference on structural faults and repairs, vol. 2; 1997. p. 109–118.

[15] Brosens K., Gemert VD. Anchoring stresses between concrete and carbon fiber reinforced laminates". In: Proceedings of 3rd Int. symposium non-metallic (frp) reinforcement for concrete structure, Sapporo, Japan Concrete Institute, vol. 1; 1997. p. 271–278.

[16] Yang YX, Yue QR, Hu YC. Experimental study on bond performance between carbon fiber sheets and concrete. J. Build Struct 2001;22(3):36–42.

[17] Ye LP, Lu XZ, Chen JF. Design proposals for the debonding strength of FRP strengthened RC beams in Chinese design code, In: Proc. of international symposium on bond behavior of FRP in structures (BBFS), Hong Kong, China; 2005. pp. 45–54.

[18] Toutanji H, Saxena P, Zhao LY, Ooi T. Prediction of interfacial bond failure of FRP-concrete surface. J Compos Constr 2007;11(4):427–36.

[19] Nehdi M, Djebbar Y, Khan A. Neural network model for preformed-foam cellular concrete. Mater J 2001;98(5):402–9.

[20] Jeon J. Fuzzy and neural network models for analyses of piles. PhD thesis, Civil, Construction and Environmental Engineering, NCSU; 2007.

[21] McCulloch Pitts WA. Logical calculus of the ideas immanent in nervous activity. J Bull Math Biophys 1993;5:115–33.

[22] Rafiq M, Bugmann G, Easterbrook D. Neural network design for engineering applications. J Comput Struct 2001;79(17):1541–52.

[23] Cladera A, Mar A. Shear design procedure for reinforced normal and high-strength concrete beams using artificial neural networks. Part II: Beams with stirrups. J Eng Struct 2004;26(7):927–36.

[24] Hajela P, Berke L. Neurobiological computational models in structural analysis and design. J Comput Struct 1991;41(4):657–67.

[25] Abdallaa JA, Elsanosib A, Abdelwahab A. Modeling and simulation of shear resistance of R/C beams using artificial neural network. J Franklin Inst 2007;344:741–56.

[26] Feng M, Bahng E. Damage assessment of jacketed RC columns using vibration tests. J Struct Eng 1999;125(3):265–71.

[27] Mukherjee A, Deshpande J, Anmada J. Prediction of buckling load of columns using artificial neural networks. J Struct Eng 1996;122(11): 1385–7.
[28] Chen S, Shah K. Neural networks in dynamic analysis of bridges. In: Proc., 8th conference on computing in civil engineering and geographic information system symposium ASCE, New York, USA, 1992. pp. 1058–1065.
[29] Feng M, Kim J. Identification of a dynamic system using ambient vibration measurements. J Appl Mech 1998;65(2):1010–23.
[30] Eldin N, Senouci A. A pavement condition-rating model using back propagation neural networks. J Microcomput Civil Eng 1995;10(6):433–41.
[31] Smith R. Principles of modeling; 2001. <http://www.modelbenders.com>.
[32] Neural network toolbox user's guide: for Use with MATLAB; 2009.
[33] Mashrei M, Abdulrazzaq N, Abdalla T, Rahman M. Neural networks model and adaptive neuro-fuzzy inference system for predicting the moment capacity of ferrocement members. J Eng Struct 2010;32(6):1723–34.
[34] Dai J, Ueda T, Sato Y. Development of the nonlinear bond stress–slip model of fiber reinforced plastics sheet–concrete interfaces with a simple method. J Compos Constr 2005;9(1):52–62.
[35] *fib*. Externally bonded FRP reinforcement for RC structures. Design and use of externally bonded fiber reinforced polymer reinforcement (FRP EBR) for reinforced concrete structures. *fib* Bulletin 14. Task group 9.3. FRP reinforcement for concrete structures. Lausanne, Switzerland; 2001.
[36] Holzenkämpfer, O. Ingenieurmodelle des verbundes geklebter bewehrung für betonbauteile. Dissertation, Technische Univ. Braunschweig, Braunschweig, Germany; 1994 [in German].
[37] CNR-DT 200. Guide for the design and construction of externally bonded FRP systems for strengthening existing structures. Rome (Italy): Italian National Research Council; 2004.
[38] Garson GD. Interpreting neural-network connection weights. J AI Expert 1991;6(7):47–51.